IUST
Iran University of Science and Technology

Iranian Journal of Electrical and Electronic Engineering

Journal Homepage: ijeee.iust.ac.ir

Research Paper

A Multi-Physics Simulation Model Based on Finite Element Method for the Multi-Layer Switched Reluctance Motor

P. Vahedi*, B. Ganji*(C.A.), and E. Afjei**

Abstract: Using ANSYS finite element (FE) package, a multi-physics simulation model based on finite element method (FEM) is introduced for the multi-layer switched reluctance motor (SRM) in the present paper. The simulation model is created totally in ANSYS parametric design language (APDL) as a parametric model usable for various conventional types of this motor and it is included electromagnetic, thermal, and structural analyses. The static characteristic of flux-linkage with a phase, phase current waveform, instantaneous torque, and electromagnetic losses are predicted using the developed electromagnetic model. Carrying out 3D FE thermal analysis, the temperature rise due to the calculated core and copper losses is predicted in the developed thermal model. The transient, modal and harmonic analyses are done in the introduced structural model to determine the mode shapes, natural frequencies, displacement, and sound pressure level (SPL) in both time and frequency domains. In order to evaluate the developed simulation model, it is applied to a typical multi-layer SRM, and simulation results related to all the above-mentioned analyses are presented.

Keywords: Multi-Layer Switched Reluctance Motor, Modeling, Electromagnetic, Thermal, Noise, Finite Element Method.

1 Introduction

NOWADAYS, the SRM has attracted much attention for industrial applications because of its rugged construction, good torque-speed characteristic, appropriate operation at high-temperature large speed conditions, and simple winding configuration. Hence, significant research has been done in three decades ago on various aspects of the conventional type of SRM including electromagnetic modeling and design [1-5], thermal modeling [6-9] and noise modeling [10-16]. In addition to the conventional types of the SRM, special topologies have been also introduced for this motor and one of these structures that can be used appropriately in some applications especially where a high power machine is needed is the multi-layer SRM [17]. In comparison to the research done on different design aspects of the conventional type of the SRM, less attention has been paid to electromagnetic modeling and design of the multi-layer SRM [18-21] and no work has been reported so far on thermal and noise modeling of this motor. Therefore, it is valuable to develop an accurate multi-physics simulation model for the multi-layer SRM by which all important analyses including electromagnetic, thermal, and noise are done.

Considering the convection heat transfer coefficients as constant parameters, a thermal analysis based on FEM is proposed in [6] for the conventional one-layer SRM. The computational fluid dynamics (CFD) analysis is used in [7] to calculate air velocity on different inner surfaces of the conventional SRM required for determination of the convection heat transfer coefficients. A thermal analysis based on FEM is introduced in [8] for the conventional SRM in which the stator structure is only considered. A thermal model based on 3D FEM is developed in [9] for the double-stator SRM in which the air-gap is assumed to be a solid material with the same major properties as air such as

Iranian Journal of Electrical and Electronic Engineering, 2020.
Paper first received 27 February 2019, revised 04 September 2019, and accepted 09 September 2019.
* The authors are with the Faculty of Electrical and Computer Engineering, University of Kashan, Kashan, Iran.
E-mails: payam_vahedi@yahoo.com and bganji@kashanu.ac.ir.
** The author is with the Faculty of Electrical Engineering, Shahid Beheshti University, Tehran, Iran.
E-mail: e-afjei@sbu.ac.ir.
Corresponding Author: B. Ganji.

thermal conductivity. Based on the structural analysis done with 2D FEM, displacement and acceleration in both time and frequency domains for the various structures of conventional SRM with 6/4 poles are predicted in [10]. In order to decrease noise of the conventional SRM, a special slot wedge referred to as structural stator spacers is introduced in [11]. Comparing noise of the 12/8 SRM and 6/4 SRM, [12] shows that the 12/8 SRM produces lower noise. Based on a thin cylinder approximation of the stator, [13] introduces a method to estimate the harmonic content of stator vibrations and acoustic noise resulting from radial force excitations in the conventional SRM. Using the structural analysis based on 3D FEM, deformation, velocity and acceleration are determined in [14] for the double-stator SRM. Based on measurement data, [15] investigates the effect of skewing the stator or/and rotor on the produced noise of the conventional SRM. In [16], mode shapes and natural frequencies of the conventional 12/8 SRM are obtained using modal analysis based on 3D FEM.

The electromagnetic analysis of a 3-layer 8/8 switched reluctance machine is presented in [17] and magnetic flux density, static torque versus rotor angle and dynamic torque are predicted. In [18], electromagnetic analysis of a novel 3-layer 4/4 SRM is presented and magnetic flux density, mutual inductance, flux linkage and static torque are determined. To decrease torque ripple of a 2-layer three-phase 6/4 SRM, a design algorithm is proposed in [19]. Using the FEM, electromagnetic modeling of a 5-layer 4/4 SRM is done in [20] to obtain the flux-linkage characteristic. Design, simulation and experimental results are presented in [21] for a novel type of 2-layer 6/4 three-phase SRM. With high-speed large-memory contemporary computer, the models based on FEM can be used appropriately these days for accurate analysis of electric machines. Therefore, the main objective of the present paper is to introduce a multi-physics simulation model based on FEM for the multi-layer SRMs. The simulation model is created totally in APDL as a parametric model and it considers all important analyses consisting of electromagnetic, thermal, and noise. In the following, the developed simulation model is described in Section 2. Applying the developed simulation model to a typical 2-layer SRM, simulation results are presented in Section 3. Finally, the paper is concluded in Section 4.

2 The Multi-Physics Simulation Model

The developed multi-physics simulation model consists of three sub-models including electromagnetic, thermal, and noise analyses. Using APDL, the model is created and it can be utilized for accurate analysis of different conventional types of multi-layer SRMs. For analysis of an electric machine with FEM using ANSYS FE package, the geometric structure of the machine needs to be plotted at first. This is a time-consuming task for a typical multi-layer SRM, especially if various designs have to be investigated. Therefore, the geometrical model of the multi-layer SRM is created in APDL as a parametric model in the developed simulation model and the numbers of stacks, stator/rotor poles, the stack length, rotor/stator poles arcs and radii of different parts are chosen as the geometrical parameters. In the following, three above-mentioned sub-models are introduced.

2.1 Electromagnetic Modeling

To carry out an electromagnetic analysis for a multi-layer SRM, it is possible to concentrate only on one layer because different layers have the same performance. For instance, similar phases in different layers of the 4-layer 8/6 SRM are excited simultaneously and the produced torque is 4 times of that in a one-layer 8/6 SRM. In addition, single-phase excitation mode is considered in the developed electromagnetic simulation model and therefore the windings areas related to one phase are only plotted in the FE model. Therefore, the procedure introduced in [22] for electromagnetic modeling of the conventional one-layer SRM is followed here to develop an electromagnetic simulation model for the multi-layer SRM. Based on static analysis in the developed simulation model, the static characteristic of flux-linkage with a phase and the static torque characteristic are determined for each layer. Carrying out the 2D FE transient analysis, the dynamic characteristics of this motor including the phase current, instantaneous torque and the flux density waveforms in different parts of the motor are also predicted in this modeling. Knowing the phase current waveform, copper losses related to the windings can be derived calculated using the below equation:

$$P_{cu} = N_l m R I_{rms}^2 \tag{1}$$

where N_l is number of layers, m is number of phases and I_{rms} is the root mean square of phase current derived from the predicted phase current waveform. Having the static characteristic of flux-linkage ($\lambda(\theta,i)$) and the instantaneous phase current ($i(\theta)$), instantaneous flux-linkage ($\lambda(\theta)$) can be determined easily. The stator pole flux waveform is obtained simply by dividing $\lambda(\theta)$ by the number of turns per phase. Using the mathematical flux model introduced in [23], flux density waveform in other parts of the magnetic circuit equivalent including stator yoke, rotor core, and rotor pole can be derived from the predicted stator pole flux waveform. Once the flux density waveform in every part of the motor is known, the following improved Steinmetz equation is considered to calculate the core loss in that part [2]:

$$P_c = K_{cf} C_h f B_{\max}^{a+bB_{\max}} + \frac{1}{2\pi^2} C_e \left(\frac{dB}{dt}\right)_{avg}^2 \tag{2}$$

where B is flux density, f is the frequency, $Bmax$ is the maximum flux density, Ch, a, b, and Ce are the Steinmetz parameters derived from the laminations datasheet and K_{cf} is modification factor for including the hysteresis losses due to minor loops.

2.2 Thermal Modeling

To predict the temperature rise in air-gap and various parts of the multi-layer SRM, a thermal model based on 3D FEM is proposed here. The SOLID90 with TEMP degree of freedom is used for all regions in the developed thermal model and both heat transfer modes including conduction and convection are considered. The effect of temperature rise on convection heat transfer coefficient is also considered in this modeling. Fig. 1 shows which type of heat transfer is considered for various surfaces in each layer. As observed in this figure, the heat transfer through the natural convection is considered for all vertical surfaces including core, end winding and shaft. In the developed simulation model, both natural and forced convection are considered for heat transfer through the frame to the surrounding air. When considering natural convection, the natural convection coefficient for a horizontal cylinder is derived as follow [8]:

$$h = \frac{k}{D} \times \left\{ 0.6 + \frac{0.387 R_{a1}^{1/6}}{\left[1 + \left(0.559 / P_r\right)^{9/16}\right]^{8/27}} \right\}^2 \tag{3}$$

where h is the heat convection coefficient, D is the outer diameter, k is the thermal conductivity of air, P_r is the Prandtl number and R_{a1} is Rayleigh number which is determined as follows:

$$R_{a1} = \frac{g \beta \left(T_s - T_a\right) D^3}{v \alpha} \tag{4}$$

where T_s is the surface temperature, T_a is the ambient temperature, β is the cubical expansion coefficient of air, α is the thermal diffusivity of air, v is the kinematic viscosity of air and g is gravitational force of attraction. For a vertical plate with diameter D, the natural convection coefficient and the Rayleigh number are estimated using the below equations:

$$h = \frac{k}{0.886 D} \times \left\{ 0.825 + \frac{0.387 R_{a2}^{1/6}}{\left[1 + \left(0.492 / P_r\right)^{9/16}\right]^{8/27}} \right\}^2,$$

$$R_{a2} = \frac{g \beta \left(T_s - T_a\right) (0.866 D)^3}{v \alpha} \tag{5}$$

The forced convection coefficient related to the inner surfaces including stator pole and slot wedge are determined as follows [8]:

$$h = \frac{0.664 k}{L} R_e^{1/2} P_r^{1/3}, \quad R_e = \frac{L v_f}{v} \tag{6}$$

where v_f is the velocity of the airflow and L is the length of the stator pole and slot wedge. In order to calculate the convection coefficient based on (3)-(6), the surfaces temperature and the surrounding air-gap temperature are required which are unknown. To solve this problem, the iterative algorithm shown in Fig. 2 is suggested in the developed thermal model. In case that air is blowed in the axial direction over the outside of the frame due to the fan, (6) can be also used to calculate the forced convection coefficient for this surface where L is the axial length of the machine [8].

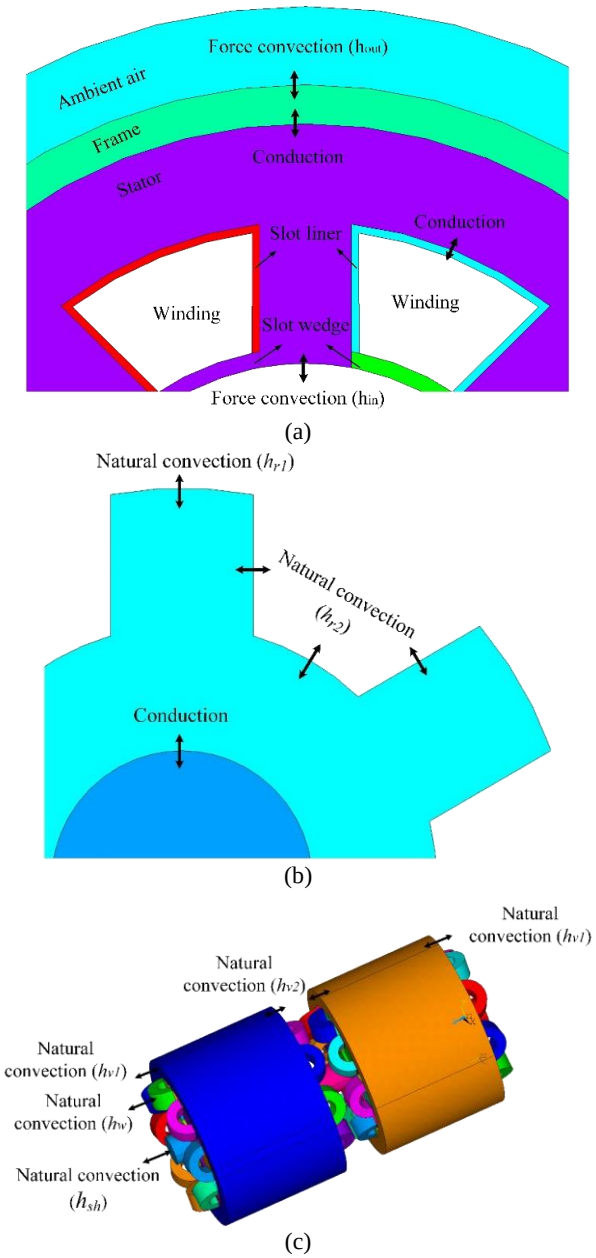

Fig. 1 Convection heat transfer through different surfaces: a) stator, b) rotor, and c) vertical surfaces.

2.3 Structural Modeling

In order to calculate noise and vibration in the multi-layer SRM, a structural model based on 3D FEM is developed which is introduced briefly in this section. The SOLID186 with Ux, Uy, and Uz degree of freedom is used in the FE model. To carry out acoustic analysis for estimation of SPL, the FLUID220 with Ux, Uy, Uz and PRES degree of freedom should be considered for the air regions. Based on the modal analysis, the natural frequencies and mode shapes of structure are determined as important parameters in the design of a structure for dynamic loading conditions. Since the stators of two adjacent layers in a multi-layer SRM have completely separate structures, their mode shapes and resonant frequency are the same. The instantaneous radial force appeared between the excited stator pole and the adjacent rotor pole is the main reason for stator vibration and acoustic noise. Carrying out 2D FE transient analysis in the developed electromagnetic model, this instantaneous radial force is predicted and it is then used for the modal analysis to determine the stator pole displacement and SPL. Based on the harmonic analysis, displacement of stator pole and SPL are also predicted in the frequency domain.

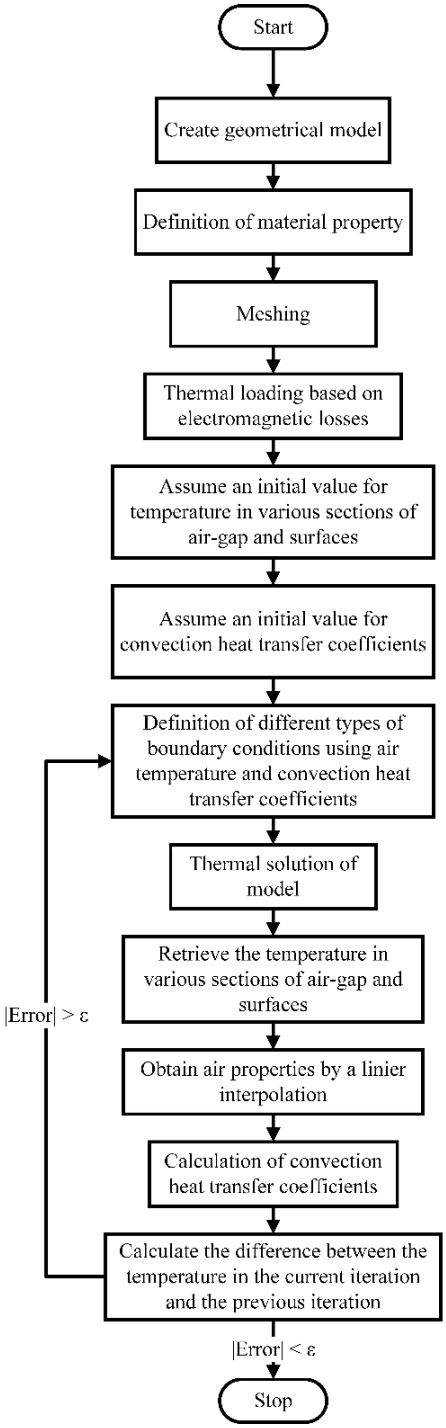

Fig. 2 Proposed thermal analysis algorithm.

3 Simulation Results

The developed multi-physics simulation model is applied to a 2-layer 8/6 SRM with the specification given in Table 1 and the simulation results are presented in this section. The geometric model of the considered motor is depicted in Fig. 3 and the laminations of stator and rotor for all layers are assumed to be M800-50A with 0.5 mm thickness. Each layer is a conventional 4-phase 8/6 SRM and the phase winding in every layer includes two coils connected together in parallel. It should be noted that all dynamic simulation results presented here are for this operating point: speed = 1000 rpm, phase voltage = 93 V, turn-on angle = 10° (mechanical degree), turn-off angle = 20° (mechanical degree) and single-pulse control mode.

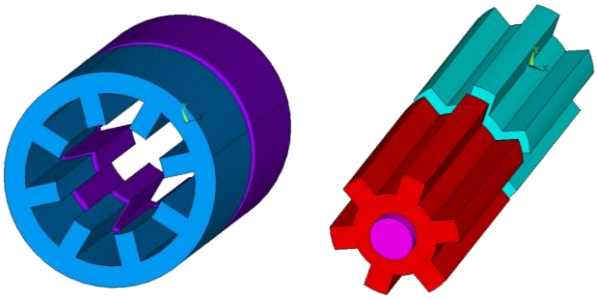

(a) (b)

Fig. 3 The structure of the considered motor: a) stator and b) rotor.

Table 1 Motor specifications

Parameter	Value
Stator outer diameter [mm]	125
Stator slot-bottom diameter [mm]	100
Rotor outer diameter [mm]	63
Rotor slot-bottom diameter [mm]	41
Air gap length [mm]	0.35
Shaft diameter [mm]	21
Stack length [mm]	90
Stator pole arc [deg.]	21
Rotor pole arc [deg.]	21
Turns per coil	124
Resistance @ 20°C [Ω]	0.69
Distance between two layers [mm]	10

Applying the developed simulation model to the discussed 2-layer SRM, the static characteristic of flux-linkage with a phase is predicted for different rotor positions and various phase currents and it is shown in Fig. 4. The computation time for each curve in this characteristic is around 75 sec on a 2.3 GHz Intel Core 2 with 10 GB RAM. Carrying out 2D FE transient analysis for the considered operating point, dynamic characteristics of the discussed 2-layer SRM including the phase current, instantaneous torque are predicted and shown in Figs. 5 and 6. Using the predicted instantaneous torque waveform, average torque and torque ripple are also determined for the considered operating point and they are 2.16 N.m and 93.74 %, respectively. The torque ripple is derived using the following equations:

$$TR\ [\%] = \frac{T_{max} - T_{min}}{2T_{av}} \times 100 \tag{7}$$

where T_{max}, $T_{min,}$ and T_{av} are maximum toque, minimum torque, and average torque, respectively.

Based on the phase voltage equation, the instantaneous phase current ($i(\theta)$) can be also determined using the predicted flux-linkage static characteristic as follows:

$$V = Ri + \frac{d\lambda(\theta, i)}{dt} \tag{8}$$

where V is phase voltage, R is phase resistance, λ is flux-linkage, θ is rotor position and i is phase current. Based on this procedure, the phase current waveform is also predicted and compared in Fig. 5 to that derived from the developed simulation model. This comparison shows well high accuracy of the developed simulation model for predicting the static characteristic of flux-linkage characteristic.

Knowing the phase current waveform ($i(\theta)$), the instantaneous torque produced by one phase ($T(\theta)$) can be determined easily from the static torque characteristic ($T(\theta,i)$). This static characteristic can be also obtained from the static characteristic of flux-linkage using the below equations.

$$w_c = \int \lambda_{(\theta,i)}\, di \tag{9}$$

$$T(\theta, i) = \frac{\partial w_c}{\partial \theta}\Big|_{i=const} \tag{10}$$

The instantaneous torque waveform of the SRM can then be derived from the instantaneous torque predicted for a phase through superposition. This curve is compared with instantaneous torque derived from simulation model (dynamic analysis) in Fig. 6. This comparison shows the accuracy of the developed simulation model for flux-linkage determination.

As indicated in Section 2.1, that it is possible to concentrate only on one layer for analysis of the multi-layer SRM because different layers have the same performance. To show this, it is necessary to evaluate the coupling effect between the similar phases in different layers on flux-linkage determination. Therefore, the flux-linkage characteristic at aligned position for two layers are derived using 3D modeling of 2-layer SRM and they are compared in Fig. 7 with

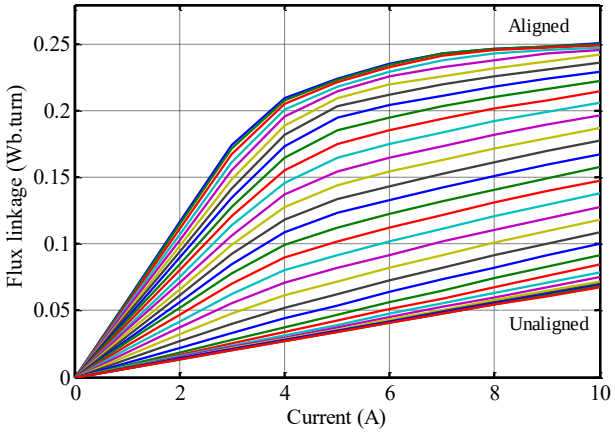

Fig. 4 The static characteristic of flux-linkage with a phase for each layer.

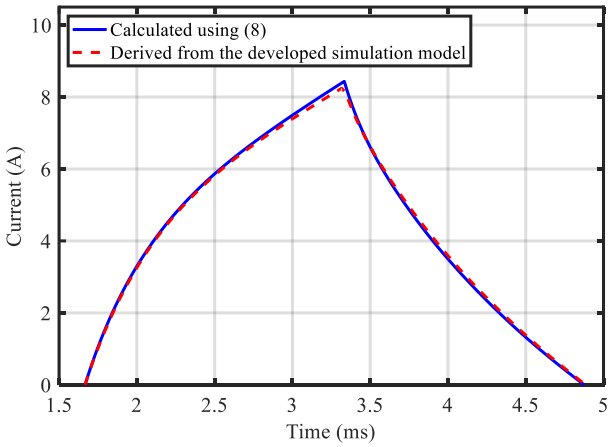

Fig. 5 The instantaneous current of one phase in each layer.

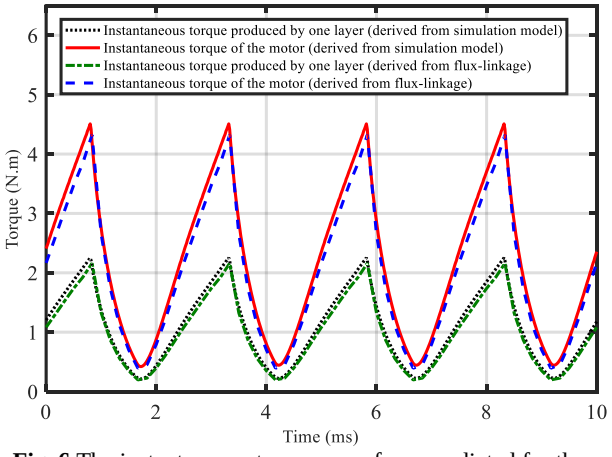

Fig. 6 The instantaneous torque waveform predicted for the considered operating point.

the flux-linkage characteristic of conventional SRM (one-layer) derived from 3D-modeling. The comparison shows well that the coupling effect between the similar phases in different layers is negligible.

The instantaneous radial force acting on stator pole, which is the main source for the stator pole displacement and noise, is also predicted for the considered operating point using the 2D FE transient analysis and it is shown in Fig. 8. In fact, this radial force is exerted on the excited stator pole from the adjacent rotor and it needs to be predicted for noise determination as done using FEM in [12]. In addition, flux density waveforms within different parts of the motor including stator pole, rotor pole, stator yoke, and rotor core are determined for the considered operating point using the developed simulation model. For instance, the flux density waveform predicted for different parts of stator yoke of the discussed 2-layer 8/6 SRM is shown in Fig. 9 and it is illustrated that the flux density waveforms are completely non-sinusoidal waveforms. Knowing the flux density waveforms in different parts of the discussed 2-layer SRM, the core loss in each part is estimated using (2) and the results are summarized in Table 2. Having the predicted phase current waveform, copper losses can be also derived from (1) and it is 43 W for the considered operating point.

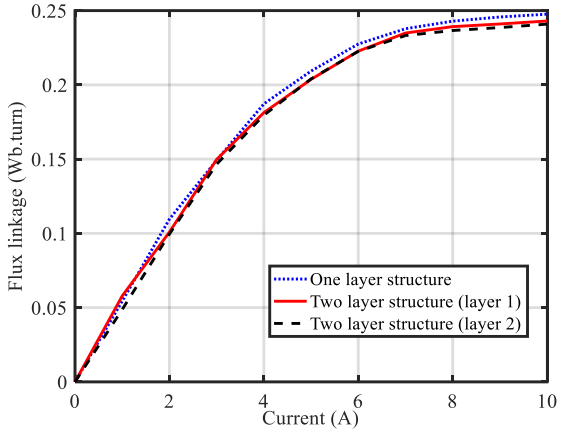

Fig. 7 The flux-linkage characteristic related to aligned position.

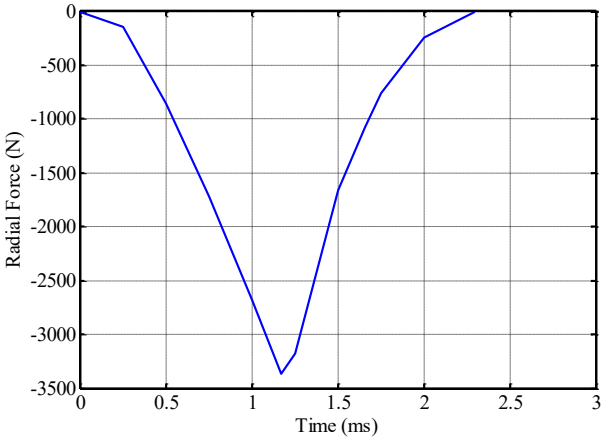

Fig. 8 The instantaneous radial force predicted for the one layer.

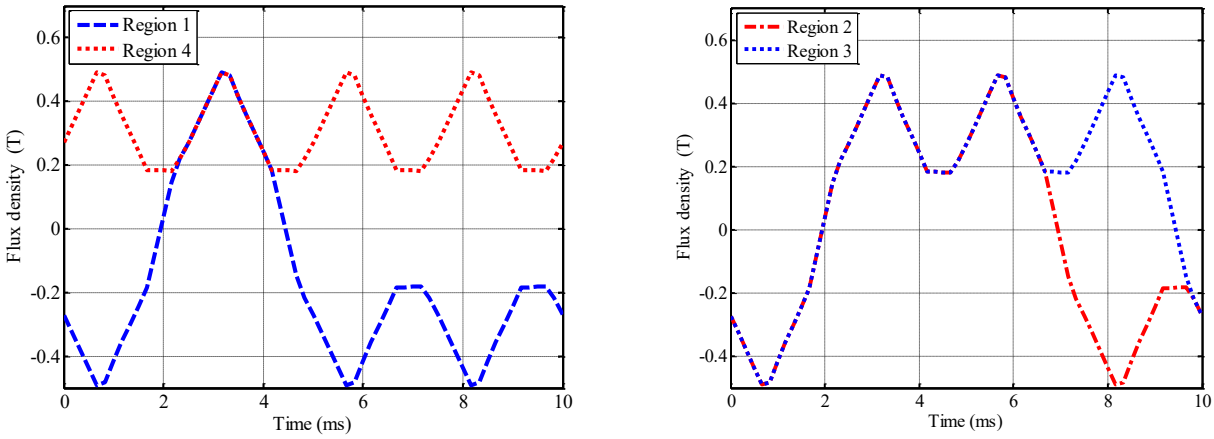

(a) (b)

Fig. 9 Flux density waveform predicted in some part of stator yoke.

Table 2 Losses calculation for the considered motor.

Core loss in stator pole [w]	9.34
Core loss in stator yoke [w]	21.02
Core loss in rotor pole [w]	3.78
Core loss in rotor yoke [w]	6.04
Copper Loss [w]	43.5

Table 3 Temperature parameters.

	Thermal conductivity [W/m/°C]	Specific heat [J/Kg/°C]	Density [Kg/m^3]
Stator lamination (iron)	20	438	7650
Copper	401	385	8933
Slot liner	0.076	1172	2150
Air	0.0263	1007	1.16
Frame (aluminium)	177	875	2770
Slot wedge	0.29	1172	2150
Shaft (steel)	14.4	461	7817

The thermal parameters used in the proposed thermal analysis are given in Table 3 and the ambient air temperature is assumed to be 20°C. Applying the algorithm depicted in Fig. 2 to the discussed 2-layer SRM, the steady-state temperature distribution for iron parts and the windings are predicted and shown in Figs. 10-11. Based on this algorithm, the steady-state temperature in air-gap, rotor yoke, stator yoke, and end winding are predicted for various iterations and the obtained values are shown in Fig. 12. Since the convection heat transfer coefficient depends on temperature, it changes in various iterations. Fig. 13 shows these variations for the coefficient related to the inner stator surface. The convection heat transfer coefficients related to different surfaces derived from the last iteration are given in Table 4. As seen obviously from Figs. 10 and 11, temperature at the space between two layers is higher than other parts and the hot spot occurs at the end-winding placed in this space. The temperature rise of various sections is derived from transient analysis and shown in Fig. 14. Effect of convection heat transfer coefficient of the outer surface on the temperature rise of the winding is also evaluated as seen in Fig. 15.

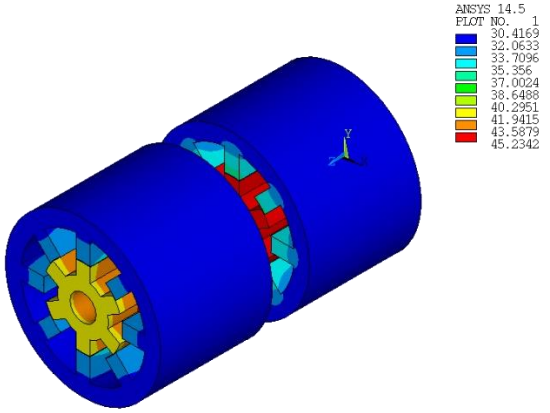

Fig. 10 Steady state temperature distribution in the core.

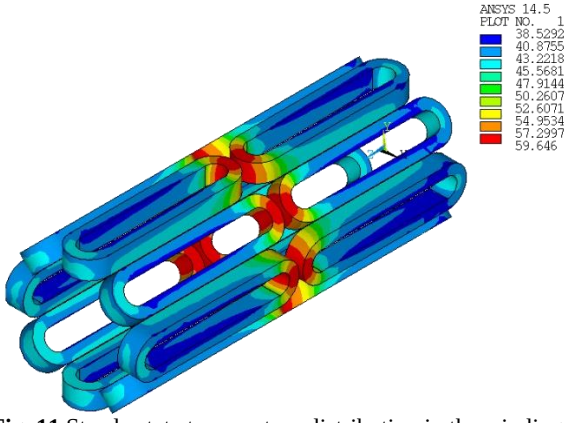

Fig. 11 Steady state temperature distribution in the windings.

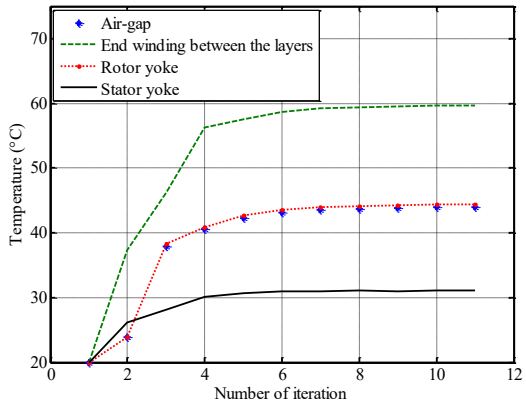

Fig. 12 Temperature in various iterations.

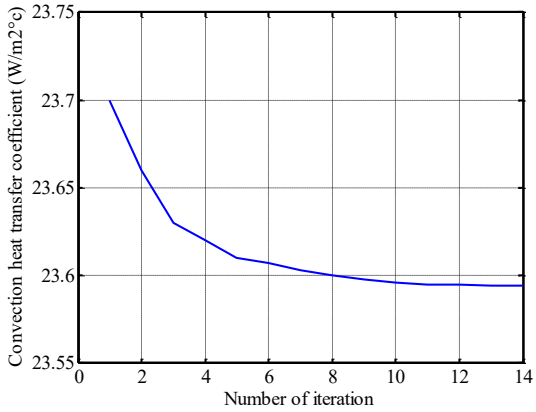

Fig. 13 Convection heat transfer coefficient for various iterations.

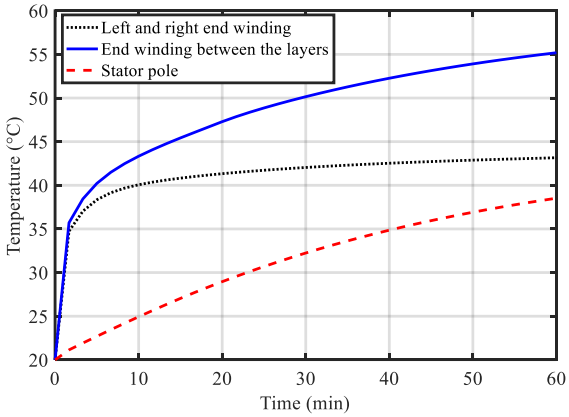

Fig. 14 Temperature rise derived from transient analysis.

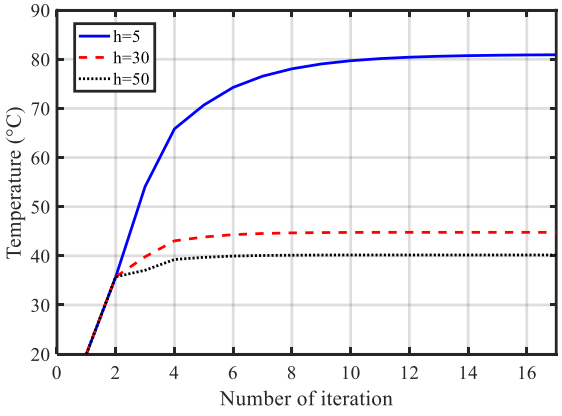

Fig. 15 Temperature rise at the middle of winding.

For the stator of the discussed 2-layer 8/6 SRM, Poisson's ratio, Young's modulus and density are 0.3, 2.07×10^{11} pa, and 7650 kg/m^3, respectively. Using the developed simulation model, the modal analysis is carried out for this motor and various mode shapes are predicted and shown in Fig. 16. In mode$_{m,n}$, m and n are number of sinewave along the longitudinal axis and circumference of the stator yoke, respectively. For the considered operating point, the stator pole displacement and the noise produced in the surrounding air are predicted and illustrated in Fig. 17. Carrying out the harmonic analysis, the stator pole displacement and SPL are also predicted in the frequency domain and they are shown in Fig. 18. With regard to this figure, the dominate mode is the mode$_{0,2}$ because it coincides with the resonant frequency of mode$_{0,2}$ illustrated in Fig. 16(a).

To evaluate impact variations of design parameters on noise of the multi-layer SRM, some design parameters including stator yoke thickness, poles arcs, stator pole height which have more effect on the noise are changed. To change these selected parameters, stator slot-bottom diameter is considered 90 mm (instead of 100 mm given in Table 1) and stator/rotor pole arcs are assumed to be 23° (instead of 21° given in Table 1). For the same instantaneous radial force (Fig. 8), noise of the

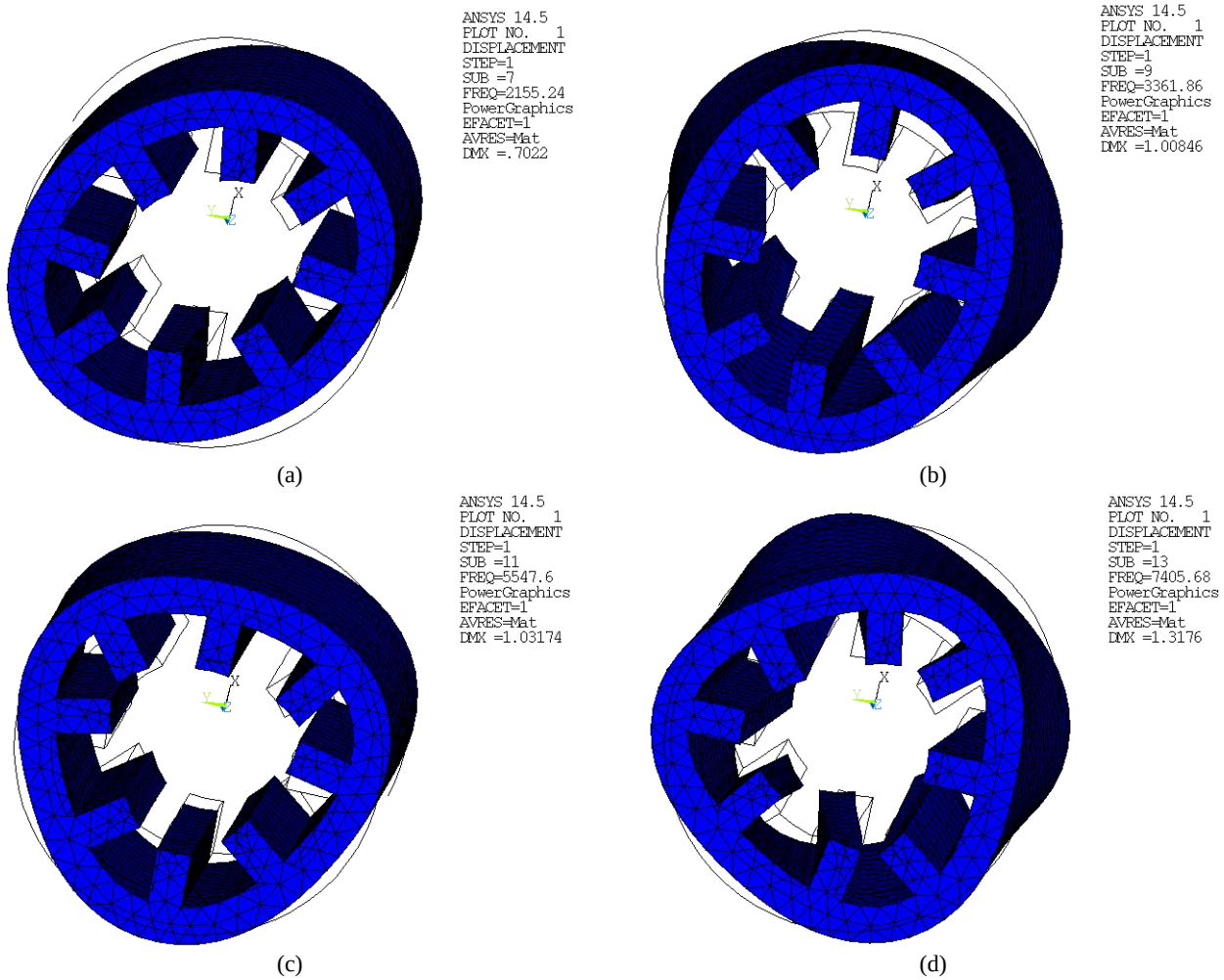

Fig. 16 Mode shapes and resonant frequency of stator of each layer from the modal analysis: a) Mode$_{0,2}$, b) Mode$_{1,2}$, c) Mode$_{0,3}$, and d) Mode$_{1,3}$.

Table 4 Convection heat transfer coefficients.

Inner stator surface (h_{in}) [w/m^2°C]	23.57
Outer stator surface (h_{out}) [w/m^2°C]	34.68
Rotor pole surface (h_{r1}) [w/m^2°C]	1.03
Rotor yoke surface (h_{r2}) [w/m^2°C]	3.2
Middle shaft surface (h_{sh3}) [w/m^2°C]	1.25
Left and right shaft surfaces (h_{sh1}) [w/m^2°C]	7.99
Left and right vertical surfaces (h_{v1}) [w/m^2°C]	4.37
Middle vertical surfaces (h_{v2}) [w/m^2°C]	1.36
End winding between the layers	8.35

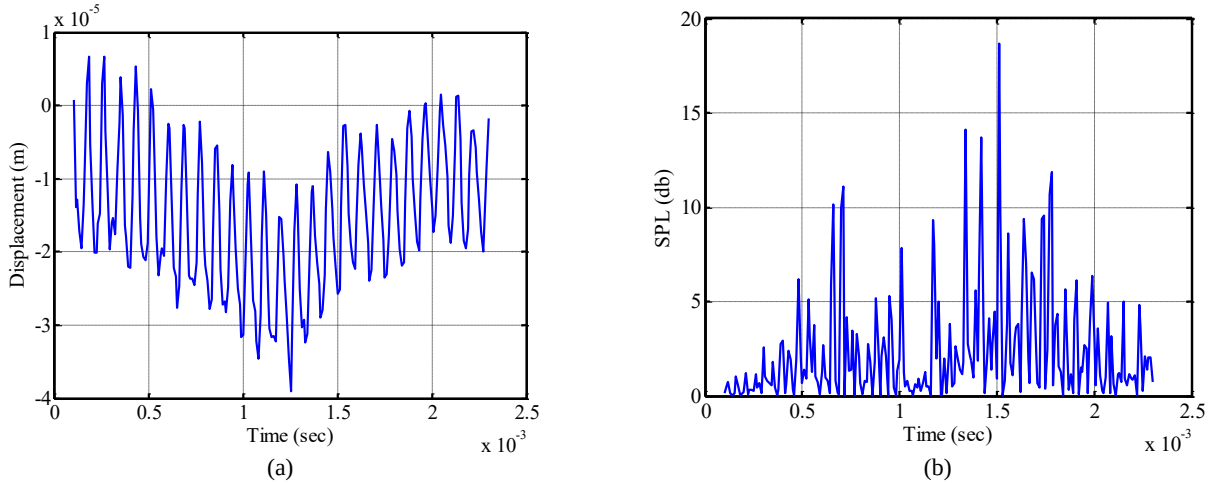

(a) (b)

Fig. 17 Simulation results for time-domain: a) the predicted stator pole displacement and b) the SPL calculated at a radius of 187 mm.

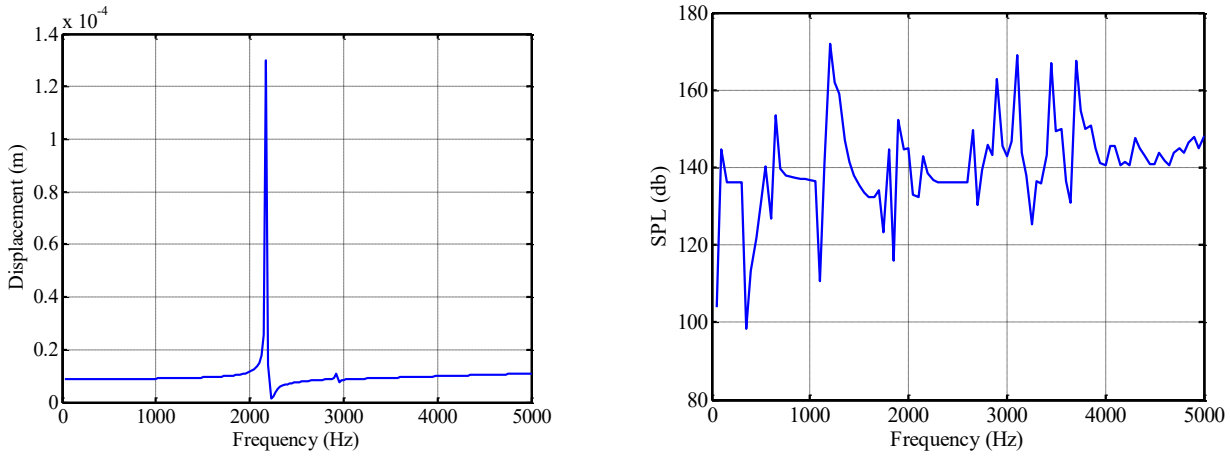

(a) (b)

Fig. 18 Simulation results for frequency domain: a) the predicted stator pole displacement and b) the calculated SPL.

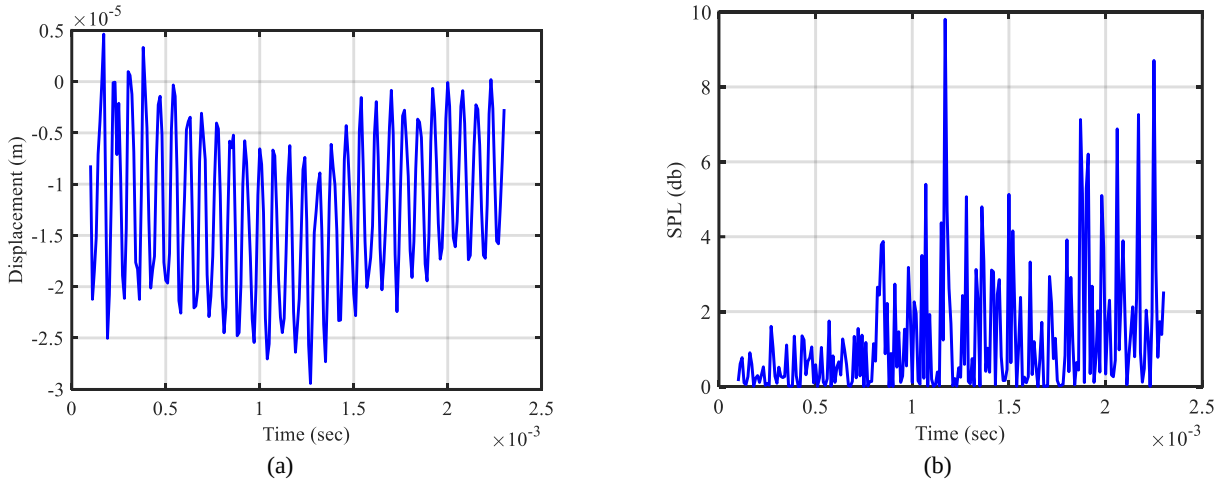

(a) (b)

Fig. 19 Simulation results for time-domain: a) the predicted stator pole displacement and b) the SPL calculated at a radius of 187 mm.

discussed 2-layer 8/6 SRM is calculated using the developed simulation model and it is illustrated in Fig. 19. Comparing Figs. 17 and 19, it is seen that noise of the motor is reduced significantly with the variations of the selected design parameters.

4 Conclusion

Based on the finite element method using ANSYS finite element package, a multi-physics simulation model for the multi-layer switched reluctance motor was introduced for the first time by which all important

analyses including electromagnetic, thermal and structural were carried out. The model has been created completely in ANSYS parametric design language as a parametric model usable for all conventional types of this motor. Applying the developed simulation model to a typical 2-layer 8/6 SRM, many simulation results included phase current, instantaneous torque, core loss, copper losses, temperature rise within the machine and the produced noise and vibration are presented for the considered operating point. As expected, the simulation results showed that the multi-layer switched reluctance motor produces higher average torque than one-layer switched reluctance motor while their torque ripple are the same. Based on the simulation results given for the developed thermal model, it was seen that the temperature at the space between two layers was higher than other sections and the end-winding placed at this space was the hot spot of the machine. With regard to the reasonable computation time of the obtained simulation results, the developed simulation model can be used properly for accurate analysis of the multi-layer switched reluctance motor because many design aspects are considered in the finite element model. Using large-memory high-speed contemporary computers, the introduced model can be also utilized appropriately for the optimal design of this motor due to consideration of electromagnetic, thermal, and structural analyses in a single platform.

References

[1] A. Radun and I. Husain, "Modeling of losses in switched reluctance machines," *IEEE Transactions on Industry Applications*, Vol. 40, No. 6, pp. 1560–1569, 2004.

[2] J. Faiz, B. Ganji, C. E. Carstensen, and R. W. DeDoncker, "Loss prediction in switched reluctance motors using finite element method," *European Transactions on Electrical Power*, Vol. 19, No. 5, pp. 731–748, 2009.

[3] W. Ding, Z. Yin, L. Liu, J. Lou, Y. Hu, and Y. Liu, "Magnetic circuit model and finite-element analysis of a modular switched reluctance machine with E-core stators and multi-layer common rotors," *IET Electric Power Applications*, Vol. 8, No. 8, pp. 296–309, 2014.

[4] Z. D. Khedda, K. Boughrara, F. Dubas, and R. Ibtiouen, "Nonlinear analytical prediction of magnetic field and electromagnetic performances in switched reluctance machines," *IEEE Transactions on Magnetics*, Vol. 53, No. 7, pp. 1–11, 2017.

[5] D. Marcsa and M. Kuczmann, "Design and control for torque ripple reduction of a 3-phase switched reluctance motor," *Computers & Mathematics with Applications*, Vol. 74, No. 1, pp. 89–95, 2017.

[6] S. Inamura, T. Sakai, and K. Sawa, "A temperature rise analysis of switched reluctance motor due to the core and copper loss by FEM," *IEEE Transactions on Magnetics*, Vol. 39, No. 3, pp. 1554–1557, 2003.

[7] K. N. Srinivas and R. Arumugam, "Analysis and characterization of switched reluctance motors: Part 2- flow, thermal and vibration analyses," *IEEE Transactions on Magnetics*, Vol. 41, No. 4, pp. 1321–1332, 2005.

[8] J. Faiz, B. Ganji, C. E. Carstensen, K. Kasper, and R. W. DeDoncker, "Temperature rise analysis of switched reluctance motors due to electromagnetic losses," *IEEE Transactions on Magnetics*, Vol. 45, No. 7, pp. 2927–2934, 2009.

[9] N. Arbab, W. Wang, C. Lin, J. Hearron, and B. Fahimi, "Thermal modeling and analysis of a double-stator switched reluctance motor," *IEEE Transactions on Energy Conversion*, Vol. 30, No. 3, pp. 1209–1217, 2015.

[10] J. P. Hong, K. H. Ha, and J. Lee, "Stator pole and yoke design for vibration reduction of switched reluctance motor," *IEEE Transactions on Magnetics*, Vol. 38, No. 2, pp. 929–932, 2002.

[11] P. Q. Rasmussen, J. H. Andreasen, and J. M. Pijanowski, "Structural stator spacers- a solution for noise reduction of switched reluctance motors," *IEEE Transactions on Industry Applications*, Vol. 40, No. 2, pp. 574–581, 2004.

[12] J. Li, X. Song, and Y. Cho, "Comparison of 12/8 and 6/4 switched reluctance motor: noise and vibration aspects," *IEEE Transactions on Magnetics*, Vol. 44, No. 11, pp. 4131–4134, 2008.

[13] J. O. Fiedler, K. Kasper, R. W. DeDoncker, "Calculation of the acoustic noise spectrum of SRM using modal superposition," *IEEE Transactions on Industry Applications*, Vol. 57, No. 9, pp. 2939–2949, 2010.

[14] A. Hasanpour and B. Fahimi, "Comparison of mechanical vibration between a double-stator switched reluctance machine and a conventional switched reluctance machine," *IEEE Transactions on Magnetics*, Vol. 50, No. 2, pp. 293–296, 2014.

[15] C. Gan, J. Wu, M. Shen, S. Yang, Y. Hu, and W. Cao, "Investigation of skewing effects on the vibration reduction of three-phase switched reluctance motors," *IEEE Transactions on Magnetics*, Vol. 51, No. 9, pp. 1–9, 2015.

[16] S. M. Castano, B. Bilgin, E. Fairall, and A. Emadi, "Acoustic noise analysis of a high-speed high-power switched reluctance machine: frame effects," *IEEE Transactions on Energy Conversion*, Vol. 31, No. 1, pp. 69–77, 2016.

[17] E. Afjei and H. Toliyat, "A novel multilayer switched reluctance motor," *IEEE Transactions on Energy Conversion*, Vol. 17, No. 2, pp. 217–221, 2002.

[18] H. Torkaman, E. Afjei, and M. S. Toulabi, "New double-layer-per-phase isolated switched reluctance motor: Concept, numerical analysis, and experimental confirmation," *IEEE Transactions on Industrial Electronics*, Vol. 59, No. 2, pp. 830–838, 2012.

[19] F. Daldaban and N. Ustkoyuncu, "Multi-layer switched reluctance motor to reduce torque ripple," *Energy Conversion and Management*, Vol. 49, No. 5, pp. 974–979, 2008.

[20] E. Afjei, A. Siadatan, and H. Torkaman, "Magnetic modeling, prototyping and comparative study of a quintuple-set switched reluctance motor," *IEEE Transactions on Magnetics*, Vol. 51, No. 8, pp. 1–7, 2015.

[21] A. Siadatan, E. Afjei, H. Torkaman, and M. Rafie, "Design, Simulation and experimental results for a novel type of two-layer 6/4 three-phase switched reluctance motor/generator," *Energy Conversion and Management*, Vol. 71, pp. 199–207, 2013.

[22] J. Faiz, B. Ganji, R. W. DeDoncker, and J. O. Fiedler, "Electromagnetic modeling of switched reluctance motor using FEM," in *32nd Annual Conference of the IEEE Industrial Electronics Society (IECON)*, pp. 1557–1562, 2006.

[23] M. Hassanin, M. T. Alrifal, and D. A. Torrey, "Experimentally verified flux density models for the switched reluctance machine," *IEEE Transactions on Magnetics*, Vol. 37, No. 5, pp. 3818–3824, 2001.

P. Vahedi was born in Shahrekord, Iran, in 1985. He received his M.Sc. in Electrical Engineering from Shahed University, Tehran, Iran, in 2010. He is currently pursuing Ph.D. degree in Electrical Engineering at the University of Kashan in Iran. Since 2013, he has been Faculty Member of the Daneshestan Nonprofit Institution of Higher Education in Iran. His main research interests include electrical machine design.

B. Ganji received B.Sc. degree from Esfahan University of Technology, Iran in 2000, and M.Sc. and Ph.D. from the University of Tehran, Iran in 2002 and 2009 respectively, all in major electrical engineering-power. He was granted DAAD scholarship in 2006 from Germany and worked in the Institute of Power Electronics and Electrical Drives at RWTH Aachen University as a visiting researcher for 6 months. He has been working at the University of Kashan in Iran since 2009 as an assistant professor and his research interest is modeling and design of advanced electric machines, especially switched reluctance motor.

E. Afjei received the B.Sc. degree in Electrical Engineering from the University of Texas at Austin, Austin, TX, USA, in 1984, the M.Sc. degree in Electrical Engineering from the University of Texas at El Paso, El Paso, TX, USA, in 1986, and the Ph.D. degree from New Mexico State University, Las Cruces, NM, USA, in 1991, He is currently a Professor of Electrical Engineering with Shahid Beheshti University, Tehran, Iran. His current research interests include switches reluctance motor drives.